Materials Chemistry and Physics 197 (2017) 154–162

Contents lists available at ScienceDirect

Materials Chemistry and Physics

journal homepage: www.elsevier.com/locate/matchemphys

Oxidation synthesis of $Hf_6Ta_2O_{17}$ superstructures

Y. Yang [a], J.H. Perepezko [a, *], C. Zhang [b]

[a] University of Wisconsin-Madison, Department of Materials Science and Engineering, 1509 University Ave., Madison, WI 53706, USA
[b] CompuTherm LLC, 8401 Greenway Blvd. Suite 248, Middleton, WI 53562, USA

HIGHLIGHTS

- Evaluation of oxidation resistance for Hf-Ta alloy with different composition.
- The Hf-26.7Ta alloy has superior oxidation resistance among all Hf-Ta alloys.
- The oxidation of the Hf-26.7Ta alloy leads to the formation of a single phase $Hf_6Ta_2O_{17}$ superstructure.
- The oxidation process leading to the synthesis of the $Hf_6Ta_2O_{17}$ superstructure has been identified.

GRAPHICAL ABSTRACT

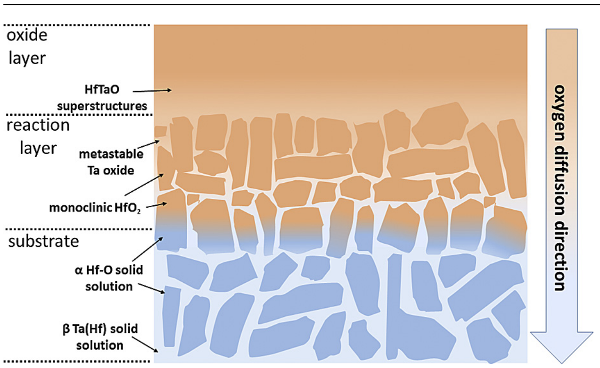

ARTICLE INFO

Article history:
Received 11 December 2016
Received in revised form
16 March 2017
Accepted 28 April 2017
Available online 3 May 2017

Keywords:
Oxide
Hf-Ta alloy
Reaction path

ABSTRACT

The microstructure evolution and phase formation sequence has been examined during the initial oxidation exposure of Hf-Ta alloys at 1500 °C for several alloy compositions. The oxidation reaction path involves the conversion of the initial β Hf-Ta BCC solid solution substrate phase into a two-phase monoclinic HfO_2 and a Ta rich BCC solid solution reaction layer that undergoes a further reaction between HfO_2 and Ta oxide to yield and outer $Hf_6Ta_2O_{17}$ superstructure. The overall reactive diffusion pathway is consistent with the calculated Hf-Ta-O ternary phase diagram. The oxidation reaction rate exhibited a minimum at Hf 26.7 at.%Ta where the outer oxide was single phase $Hf_6Ta_2O_{17.}$ For other compositions the outer oxide was composed of $Hf_6Ta_2O_{17}$ and either HfO_2 (Hf-rich compositions) or Ta_2O_5 (Ta-rich compositions). The enhanced oxidation resistance for the Hf-26.7 at.%Ta alloy is attributed to the adherent $Hf_6Ta_2O_{17}$ superstructure.

© 2017 Elsevier B.V. All rights reserved.

1. Introduction

The heightened interest in energy generation and efficiency has highlighted the long standing importance of the role of high temperature ceramic materials that exhibit reliable performance in aggressive environments. Under such demanding service conditions the clear choice for a robust material is based upon oxides. As the drive for higher temperature use continues, the number of available materials shrinks drastically; especially for temperatures of 2000 °C and above. Materials for ultrahigh temperature environments must satisfy several stringent requirements that dictate a high melting temperature and stability in an oxidizing environment that often contains water vapor as well as other compatibility issues. While a few candidates have been identified such as zirconates [1], sialons [2] and diborides [3], most of the recent attention has been focused on diborides (ZrB_2 and HfB_2) for

---

* Corresponding author.
E-mail address: perepezk@engr.wisc.edu (J.H. Perepezko).

http://dx.doi.org/10.1016/j.matchemphys.2017.04.055
0254-0584/© 2017 Elsevier B.V. All rights reserved.

ultrahigh temperatures due to a number of attributes such as favorable mechanical and thermal properties [3]. However, the diborides do not exhibit acceptable oxidation behavior as monolithic material since the oxidation reaction at high temperature yields a volatile B_2O_3 and a porous oxide skeleton (i.e. ZrO_2 or HfO_2). In order to achieve an enhancement of the oxidation resistance a number of different additives have been examined with the aim of altering the defect structure of ZrO_2 [4] or modifying the constitution of the oxide scale (i.e. by promoting a phase separation and increased viscosity) [5]. While there have been some improvements with these approaches, the oxidation attack is still significant and limits the service life.

What is needed for enhanced high temperature capability are new materials either in the form of new oxides or new surface coatings. There are a large number of ternary and higher order oxides involving two or more metal components. The multicomponent oxide structures develop at much higher additive levels than those typically involved in doping, but the structural modifications can also have a significant impact on oxygen transport. For example, in the case of transition metals, the characteristic multiple valence states are associated with different oxide structures. This characteristic behavior suggests a possible route to identify new high temperature oxides that can also inhibit oxygen transport in ultrahigh temperature ceramics.

In the case of Hf-Ta, an early report by Marnoch [6] on the oxidation of Hf-Ta alloys provided some intriguing results on enhancing oxidation resistance. The Hf-Ta system [7] is characterized by a monotectoid isotherm reaction at 1083 °C and 46.8 at. % Ta. At elevated temperature, there is a miscibility gap in the BCC phase. The melting points for Hf and Ta are respectively, 2231 °C and 3020 °C. Marnoch [6] reported that, with increasing alloying levels of Ta, Hf-Ta alloys exhibited an increasing oxidation resistance up to 27 wt.% Ta based upon metallographic study of oxidized sample cross sections. However, neither the oxide structure nor the kinetic behavior were determined completely.

During the oxidation of Hf [8–10], the oxidation product is monoclinic HfO_2 above 550 °C. The oxidation of Ta [11,12] involves an initial oxygen dissolution, formation of intermediate suboxides, such as tetragonal TaO_z below 800 °C and TaO from 800 °C to 1000 °C, then finally formation of Ta_2O_5. Above 800 °C, the oxidation of Ta first exhibits parabolic kinetic behavior and then transforms to a linear oxidation rate due to the cracking of the Ta_2O_5 oxide scale. Based upon the reported oxidation behavior for Hf and Ta it is puzzling that the oxidation resistance for Hf-Ta alloys reaches a maximum at Hf- 27 wt. % Ta solely due to HfO_2 or Ta_2O_5 as an external protective scale. Moreover, recently, Hf-based metallic coatings have been successfully applied to carbon composites where the oxidation resistance up to 1850 °C is dramatically increased by 27 wt. % tantalum addition [13]. It is not clear however as to the mechanism by which tantalum can be added into Hf-based known oxides (monoclinic, tetragonal as well as cubic) as there is very limited available data on the plethal section for $HfO_2 - Ta_2O_5$. In addition, Spridonov et al. [14] reported a series of homologous superstructures, in which the chemical formula can be represented by $xHfO_2 \cdot Ta_2O_5$ ($x = 5, 6, 7$) with a ratio of Hf:Ta (2.5:1–3.5:1. hereafter, identified as HfTaO superstructures.), which possess an orthorhombic crystal structure and share similar X-ray diffraction patterns. However, for a very similar orthorhombic ZrNbO superstructure, there is another explanation [15,16], in which the superstructure is treated as incommensurate superstructure and the chemical formula for this superstructure is represented as $Zr_{x-2}Nb_2O_{2x+1}$ ($x = 7.1–10.3$). Sine there is still a need to refine the crystal structure of the HfTaO superstructures, we will treat them as a common structure with some composition range rather than differentiate them.

In this study, the sequence of oxidation steps in Hf-Ta alloys has been identified in order to determine the oxidation product of the Hf- 26.7 wt. % Ta alloy, The oxidation reaction exhibits both an internal oxidation and the formation of an external scale behavior. Moreover, the oxidation leads to the conversion of the monoclinic HfO_2 into an oxide superstructure based upon $Hf_6Ta_2O_{17}$ that is identified as the source for the improvement in the oxidation resistance.

2. Materials and method

The Hf-Ta alloys with compositions of Hf-19.7Ta, Hf-26.7Ta, Hf-34.7Ta and Hf-49.6Ta (all compositions reported are in atomic percent unless otherwise stated) were fabricated by arc melting from pure hafnium (99.7%, Zr nominal 3%, Alfa Aesar Inc. MA. U.S.) and pure tantalum (99.95%, Alfa Aesar Inc. MA. U.S.). The resulting ingots were homogeneous with grain sizes of about 400 μm. Oxidation samples were sliced from alloy ingots with a thickness of about 1.5 mm. The alloy microstructures were examined under a ZEISS LEO-1530 scanning electron microscope (SEM) operating at 20 kV. All images were taken in the backscattering electron (BSE) mode, which reflects the composition contrast in the samples. The reaction layer thickness measurement was performed with imageJ software. The X-Ray diffraction (XRD) patterns were acquired in a Bruker D8 Advanced diffractometer using a Cu $K\alpha$ (wavelength 1.54 Å) source to determine the phases present. An area detector was used to collect the diffraction data; the exposition time was one minutes per frame and a diffraction pattern was collected from four frames.

Before oxidation, samples were polished to 1 μm with a diamond suspension and cleaned in acetone. The as cast alloys were characterized by XRD. For the Hf- 19.7Ta alloy, the sample is a α Hf-Ta solid solution with a hexagonal crystal structure while for alloys with other compositions, the samples were characterized as metastable β Hf-Ta solid solutions with a body-centered cubic (BCC) crystal structure. For oxidation exposure, the samples were loaded in an alumina boat and placed in a preheated furnace at 1500 °C for 10 min in laboratory air. The sample compositions and oxidation conditions are labeled in the Hf-Ta binary phase diagram shown in Fig. 1. From the phase diagram, it is evident that all selected Hf-Ta alloys at 1500 °C are equilibrium β Hf-Ta solid solutions.

The crystal structure of the oxide scale for each sample was determined by XRD. All samples after oxidation were cut normal to the surface and polished to 1 μm to examine the microstructures in cross section. To investigate the oxidation sequences, an oxidized Hf-26.7Ta sample was polished carefully along the oxygen diffusion direction (normal to the surface). After each increment of polishing, the phases present were determined by XRD and the microstructure was characterized by SEM. Moreover, for another oxidized Hf-

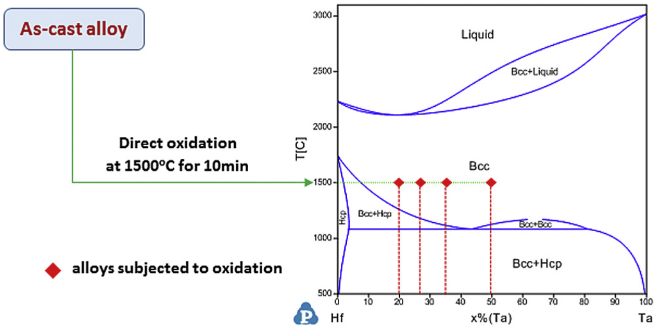

Fig. 1. Hf-Ta phase diagram and sample illustration.

Download English Version:

https://daneshyari.com/en/article/5447985

Download Persian Version:

https://daneshyari.com/article/5447985

Daneshyari.com